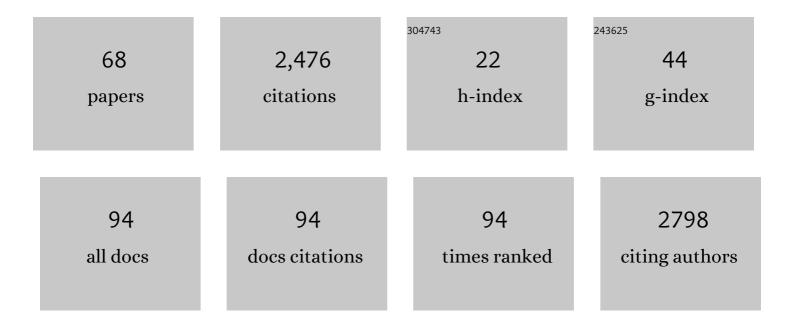
## Andreas Fix

List of Publications by Year in descending order

Source: https://exaly.com/author-pdf/8530821/publications.pdf Version: 2024-02-01



ANDREAS FIX

#	Article	IF	CITATIONS
1	Depolarization ratio profiling at several wavelengths in pure Saharan dust during SAMUM 2006. Tellus, Series B: Chemical and Physical Meteorology, 2022, 61, 165.	1.6	436
2	Aerosol classification by airborne high spectral resolution lidar observations. Atmospheric Chemistry and Physics, 2013, 13, 2487-2505.	4.9	209
3	Airborne high spectral resolution lidar for measuring aerosol extinction and backscatter coefficients. Applied Optics, 2008, 47, 346.	2.1	142
4	ACRIDICON–CHUVA Campaign: Studying Tropical Deep Convective Clouds and Precipitation over Amazonia Using the New German Research Aircraft HALO. Bulletin of the American Meteorological Society, 2016, 97, 1885-1908.	3.3	124
5	Permafrost carbon emissions in a changing Arctic. Nature Reviews Earth & Environment, 2022, 3, 55-67.	29.7	124
6	ML-CIRRUS: The Airborne Experiment on Natural Cirrus and Contrail Cirrus with the High-Altitude Long-Range Research Aircraft HALO. Bulletin of the American Meteorological Society, 2017, 98, 271-288.	3.3	107
7	The North Atlantic Waveguide and Downstream Impact Experiment. Bulletin of the American Meteorological Society, 2018, 99, 1607-1637.	3.3	105
8	Evidence for inertia gravity waves forming polar stratospheric clouds over Scandinavia. Journal of Geophysical Research, 2002, 107, SOL 30-1.	3.3	103
9	MERLIN: A French-German Space Lidar Mission Dedicated to Atmospheric Methane. Remote Sensing, 2017, 9, 1052.	4.0	88
10	EUREC <sup>4</sup> A. Earth System Science Data, 2021, 13, 4067-4119.	9.9	88
11	CHARM-F—a new airborne integrated-path differential-absorption lidar for carbon dioxide and methane observations: measurement performance and quantification of strong point source emissions. Applied Optics, 2017, 56, 5182.	2.1	87
12	On the onset of bora and the formation of rotors and jumps near a mountain gap. Quarterly Journal of the Royal Meteorological Society, 2008, 134, 21-46.	2.7	80
13	Spatial distribution and optical properties of Saharan dust observed by airborne high spectral resolution lidar during SAMUM 2006. Tellus, Series B: Chemical and Physical Meteorology, 2022, 61, 131.	1.6	71
14	Low stratospheric water vapor measured by an airborne DIAL. Journal of Geophysical Research, 1999, 104, 31351-31359.	3.3	44
15	Optical parametric oscillators and amplifiers for airborne and spaceborne active remote sensing of CO2 and CH4. Proceedings of SPIE, 2011, , .	0.8	44
16	Latent heat flux measurements over complex terrain by airborne water vapour and wind lidars. Quarterly Journal of the Royal Meteorological Society, 2011, 137, 190-203.	2.7	42
17	Quantifying CH <sub>4</sub> emissions from hard coal mines using mobile sun-viewing Fourier transform spectrometry. Atmospheric Measurement Techniques, 2019, 12, 5217-5230.	3.1	38
18	Estimating CH <sub>4</sub> , CO <sub>2</sub> and CO emissions from coal mining and industrial activities in the Upper Silesian Coal Basin using an aircraft-based mass balance approach. Atmospheric Chemistry and Physics, 2020, 20, 12675-12695.	4.9	36

ANDREAS FIX

#	Article	IF	CITATIONS
19	Upconversion-based lidar measurements of atmospheric CO_2. Optics Express, 2016, 24, 5152.	3.4	31
20	Crosslinking of progesterone receptor to DNA using tuneable nanosecond, picosecond and femtosecond UV laser pulses. Nucleic Acids Research, 1997, 25, 2478-2484.	14.5	30
21	Potential of airborne lidar measurements for cirrus cloud studies. Atmospheric Measurement Techniques, 2014, 7, 2745-2755.	3.1	29
22	How stratospheric are deep stratospheric intrusions? LUAMIÂ2008. Atmospheric Chemistry and Physics, 2016, 16, 8791-8815.	4.9	29
23	Atmospheric CO\$_2\$ Sensing with a Random Modulation Continuous Wave Integrated Path Differential Absorption Lidar. IEEE Journal of Selected Topics in Quantum Electronics, 2017, 23, 157-167.	2.9	24
24	Upconversion detector for range-resolved DIAL measurement of atmospheric CH <sub>4</sub> . Optics Express, 2018, 26, 3850.	3.4	24
25	Error Budget of the MEthane Remote LIdar missioN and Its Impact on the Uncertainties of the Global Methane Budget. Journal of Geophysical Research D: Atmospheres, 2018, 123, 11,766.	3.3	23
26	Airborne high spectral resolution lidar observation of pollution aerosol during EUCAARI-LONGREX. Atmospheric Chemistry and Physics, 2013, 13, 2435-2444.	4.9	22
27	Analysis of a potential-vorticity streamer crossing the Alps during MAP IOP 15 on 6 November 1999. Quarterly Journal of the Royal Meteorological Society, 2003, 129, 609-632.	2.7	18
28	Estimating Upper Silesian coal mine methane emissions from airborne in situ observations and dispersion modeling. Atmospheric Chemistry and Physics, 2021, 21, 8791-8807.	4.9	18
29	Validation of MIPAS-ENVISAT H <sub>2</sub> O operational data collected between July 2002 and March 2004. Atmospheric Chemistry and Physics, 2013, 13, 5791-5811.	4.9	17
30	Potential of Spaceborne Lidar Measurements of Carbon Dioxide and Methane Emissions from Strong Point Sources. Remote Sensing, 2017, 9, 1137.	4.0	16
31	Quantification of CH <sub>4</sub> coal mining emissions in Upper Silesia by passive airborne remote sensing observations with the Methane Airborne MAPper (MAMAP) instrument during the CO <sub>2</sub> and Methane (CoMet) campaign. Atmospheric Chemistry and Physics. 2021, 21, 17345-17371.	4.9	16
32	Influence of molecular scattering models on aerosol optical properties measured by high spectral resolution lidar. Applied Optics, 2009, 48, 5143.	2.1	15
33	In situ observations of greenhouse gases over Europe during the CoMet 1.0 campaign aboard the HALO aircraft. Atmospheric Measurement Techniques, 2021, 14, 1525-1544.	3.1	15
34	Development and application of an airborne differential absorption lidar for the simultaneous measurement of ozone and water vapor profiles in the tropopause region. Applied Optics, 2019, 58, 5892.	1.8	14
35	Hindcasting and forecasting of regional methane from coal mine emissions in the Upper Silesian Coal Basin using the online nested global regional chemistry–climate model MECO(n) (MESSy v2.53). Geoscientific Model Development, 2020, 13, 1925-1943.	3.6	14
36	CoMet: an airborne mission to simultaneously measure CO2 and CH4 using lidar, passive remote sensing, and in-situ techniques. EPJ Web of Conferences, 2018, 176, 02003.	0.3	13

ANDREAS FIX

#	Article	IF	CITATIONS
37	Determination of the emission rates of CO <sub>2</sub> point sources with airborne lidar. Atmospheric Measurement Techniques, 2021, 14, 2717-2736.	3.1	13
38	Injection-seeded optical parametric oscillator for airborne water vapour DIAL. Journal of Optics, 1998, 7, 837-852.	0.5	11
39	Investigations on the beam pointing stability of a pulsed optical parametric oscillator. Optics Express, 2013, 21, 10720.	3.4	9
40	Denitrification inside the stratospheric vortex in the winter of 1999–2000 by sedimentation of large nitric acid trihydrate particles. Journal of Geophysical Research, 2002, 107, AAC 11-1.	3.3	8
41	Energy calibration of integrated path differential absorption lidars. Applied Optics, 2018, 57, 7501.	1.8	8
42	Compact, passively Q-switched, all-solid-state master oscillator-power amplifier-optical parametric oscillator (MOPA-OPO) system pumped by a fiber-coupled diode laser generating high-brightness, tunable, ultraviolet radiation. Applied Optics, 2009, 48, 3839.	2.1	7
43	Detection and Analysis of Water Vapor Transport by Airborne Lidars. IEEE Journal of Selected Topics in Applied Earth Observations and Remote Sensing, 2013, 6, 1189-1193.	4.9	7
44	INNOSLAB-based single-frequency MOPA for airborne lidar detection of CO2and methane. , 2014, , .		7
45	Fast-switching system for injection seeding of a high-power Ti:sapphire laser. Review of Scientific Instruments, 2009, 80, 073110.	1.3	6
46	Mixing at the extratropical tropopause as characterized by collocated airborne H <sub>2</sub> O and O <sub>3</sub> lidar observations. Atmospheric Chemistry and Physics, 2021, 21, 5217-5234.	4.9	6
47	Development and First Results of a new Near-IR Airborne Greenhouse Gas Lidar. , 2015, , .		4
48	Feasibility and performance study for a space-borne 1645nm OPO for French-German satellite mission MERLIN. , 2014, , .		3
49	Measurement characteristics of an airborne microwave temperature profiler (MTP). Atmospheric Measurement Techniques, 2021, 14, 1689-1713.	3.1	3
50	Tunable Light Sources for Lidar Applications. Research Topics in Aerospace, 2012, , 509-527.	0.7	3
51	Depolarization ratio profiling at several wavelengths in pure Saharan dust during SAMUM 2006. Tellus, Series B: Chemical and Physical Meteorology, 2009, 61, .	1.6	3
52	Investigations on frequency and energy references for a space-borne integrated path differential absorption lidar. , 2017, , .		3
53	Feasibility and performance study for a space-borne 1645 nm OPO for French-German satellite mission MERLIN. Proceedings of SPIE, 2014, , .	0.8	2
54	Airborne Differential Absorption and High Spectral Resolution Lidar Measurements for Cirrus Cloud Studies. EPJ Web of Conferences, 2016, 119, 11003.	0.3	2

		_
- Λ NI	DREAS	
	DKEAS	

#	Article	IF	CITATIONS
55	Challenges and Solutions for Frequency and Energy References for Spaceborne and Airborne Integrated Path Differential Absorption Lidars. EPJ Web of Conferences, 2016, 119, 06012.	0.3	2
56	On the benefit of airborne demonstrators for space borne lidar missions. , 2017, , .		2
57	Development and First Results of a new Near-IR Airborne Greenhouse Gas Lidar. , 2015, , .		2
58	<title>Injection-seeded optical parametric oscillator for airborne DIAL</title> ., 1997, , .		1
59	Water vapour and wind profiles from collocated airborne lidars during COPS 2007. Proceedings of SPIE, 2007, 6750, 207.	0.8	1
60	Airborne lidar observations of water vapor transport. , 2012, , .		1
61	OPO resonator length stabilisation for injection seeding using fibre coupled heterodyne detection. , 2008, , .		1
62	CH4 and CO2 IPDA Lidar Measurements During the Comet 2018 Airborne Field Campaign. EPJ Web of Conferences, 2020, 237, 03005.	0.3	1
63	<title>Design and performance of efficient narrowband and mode-locked optical parametric oscillators of BBO and KTP</title> . , 1993, , .		0
64	Spectral purity investigation of a KTP optical parametric oscillator. , 2006, , .		0
65	Airborne measurements of ground reflectance at 1.6 î¼m. Proceedings of SPIE, 2008, , .	0.8	0
66	Performance of Charm-F – the airborne demonstrator for Merlin. EPJ Web of Conferences, 2018, 176, 01002.	0.3	0
67	Upconversion-based lidar measurements of atmospheric CO2. , 2016, , .		0

68 Upconversion Detector for Methane Atmospheric Sensor. , 2017, , .

0